JOURNAL OF MOLECULAR SPECTROSCOPY 3, 299–334 (1959)

Rotation Spectrum of Methyl Alcohol*

DONALD G. BURKHARD† AND DAVID M. DENNISON

Randall Laboratory of Physics, The University of Michigan, Ann Arbor, Michigan

The rotation spectrum of methanol vapor has been measured from 50 to 457 cm^{-1}. Combining these data with the work of Borden and Barker provides an accurate map of the spectrum to 625 cm^{-1} together with some provisional observations between 695 and 860 cm^{-1}. The primary purpose of the theoretical discussion is to identify the observed lines and subsequently, through combination relations, to establish the rotational energy levels of the molecule. These levels may be labeled by the quantum number n, τ, K, and J. n corresponds roughly to a vibration in the hindering potential field and τ designates the three types of levels resulting from the threefold potential. J gives the total angular momentum and K its component along the molecular symmetry axis.

The method of analysis consisted first in calculating the rotational levels using the barrier height and the moments of inertia established through earlier investigations of the microwave spectrum. The intensities of the lines occurring within the region of experimental observation were calculated. The resulting predicted spectrum when compared with the observed spectrum allowed a considerable number of identifications to be made but revealed deviations due to centrifugal force effects. These latter were then calculated and ultimately a very satisfactory fit was obtained. The rotational levels were then determined for $n = 0, 1, 2$, and 3 and for $K = 0$ through 10. The accuracy is estimated to be of the order of a few tenths of a wave per centimeter. The small discrepancies between these observed levels and the calculated levels (taking account of centrifugal distortion) are discussed and it is concluded that the hindering potential must be sinusoidal in form with an accuracy of better than one percent.

INTRODUCTION

The rotation spectrum of methanol is one of the most complex, intense and extensive spectra which has been studied. Its complexity arises from the phenomenon of internal rotation and from the fact that the hindering barrier is comparable with the thermal energy kT. It is intense since the molecule possesses

* This work has been supported in part by Army Ordnance Research, by the Petroleum Research Fund administered by the American Chemical Society, and by the Office of Naval Research.

† Present address: Department of Physics, University of Colorado, Boulder, Colorado.

a relatively large component of permanent electric moment in a direction perpendicular to the symmetry axis, namely, $\mu_\perp = 1.44 \times 10^{-18}$ esu. Finally it is very extensive since the moment of inertia of one of the rotating components, namely that of the hydroxyl group, is small, thus allowing the existence of high rotational frequencies.

The early observations of the rotation spectrum were made by Borden and Barker (*1*) who measured the absorption from 380 cm^{-1} to 624 cm^{-1} and from 695 cm^{-1} to 860 cm^{-1}. The exclusion of the middle region was due to presence of the strong carbon dioxide band at 667 cm^{-1}. At the higher frequencies Borden and Barker found the spectrum to be relatively simple and to consist of groups of lines with a spacing of around 40 cm^{-1} which they somewhat correctly attributed to a free rotation of the hydroxyl group although the connection is not as simple as originally supposed. As they proceeded towards longer wavelengths they observed that the lines became more numerous and their spacing highly irregular, a feature which is fully corroborated by the present investigation which extends the measurement to 50 cm^{-1}. In the region from 150 to 300 cm^{-1} the lines are so intense and so crowded together that it has proved difficult to fully resolve them. Below 150 cm^{-1} their intensity diminishes somewhat although the general complexity of the spectrum remains high.

A theory of the rotational spectrum of methanol was developed by Koehler and Dennison (*2*) using a simplified model to represent the molecule. This theory predicted a highly irregular and intense spectrum in accord with observation but it was not possible to identify the individual rotational lines and hence to calculate the height of the potential barrier. No further progress was made until 1947 when a series of related lines was found by Hershberger and Turkevich (*3*) in the microwave spectrum of methanol. These lines were later observed with great accuracy by Hughes *et al.* (*4*) who measured their Stark effect. This allowed a unique identification of the lines and the subsequent analyses of Burkhard *et al.* (*5*, *6*) led to a convincing number of internal checks together with a determination of a barrier height of 374.8 cm^{-1}.

The present paper consists of two parts: (a) an experimental measurement of the methanol spectrum out to 50 cm^{-1} and (b) an attempt to identify the lines and to obtain the rotational energy levels of the molecule. In carrying out the identification, difficulties were encountered similar to those found in analyzing the complex spectrum of water vapor and due essentially to the same causes. Since the moment of inertia of the hydroxyl group is small and the potential barrier relatively low, the resulting rotational frequencies are high. The centrifugal forces are correspondingly large and produce distortions in the molecule which may shift the lines by as much as several waves per centimeter. Shifts of this magnitude in a crowded spectrum often make the identifications ambiguous. The methods which were employed in making the analysis contained the following elements: (1) a calculation of the rotational energy levels of the molecule

neglecting centrifugal distortion; (2) an approximate calculation of the effect of centrifugal distortion; (3) a calculation of the intensities of the lines and (4) the use of combination relations to confirm provisional identifications. It will be considered that a given energy level has been established only when it satisfies the following two criteria. First, all principal transitions to previously established levels must correspond to observed spectral lines. The predicted and measured intensities must be in good qualitative agreement and the discrepancies between their predicted and measured positions must not exceed a few tenths of a wave per centimeter. This figure arises partly from experimental and partly from theoretical considerations and will be discussed later. The second criterion is that the given level, when allowance is made for centrifugal distortion, must fit into the pattern of energy levels predicted by the theory of hindered rotation.

2. EXPERIMENTAL

The large grating spectrometer designed by Randall and Firestone (*7*) was used for the infrared measurements. In order to cover the complete range from 22μ to 200μ the following gratings were used in the regions indicated.

50 cm^{-1} to 106 cm^{-1}	87 lines per inch
91 cm^{-1} to 148 cm^{-1}	133 lines per inch
122 cm^{-1} to 225 cm^{-1}	360 lines per inch
180 cm^{-1} to 323 cm^{-1}	600 lines per inch
297 cm^{-1} to 457 cm^{-1}	900 lines per inch.

Filtering and restrahlen combinations were essentially the same as those recommended by Fuson (*8*). In general it seemed to be possible to get pure records in the far infrared region with less quartz and wax than Fuson found necessary. It appears likely that the temperature of the source used in the present work was lower than the temperature of the source used by Fuson.

Grating constants were obtained by calibrating the instrument against water lines (*9*). Water lines were also used as a constant check on the degree of resolution and purity. Resolution was very good at all times. The spectrometer was refocused at the time the work was started.

Each region was run at least three times with different pressures and slit widths, and one continuous run was made over the whole region using methyl alcohol at a constant pressure.

In order to utilize all available energy and eliminate the energy losses which would occur if a cell were used, the methyl alcohol was introduced directly into the main body of the spectrometer. The vapor was kept out of the source box by a thin film of polythene (approximately 1μ thickness), while studying the region from 22μ to 40μ. This material was found to be very durable, unaffected

by methyl alcohol and highly transparent in this region. It transmitted eighty-five to ninety percent of the radiation. From 40μ to 200μ a quartz window was placed between the grating chamber and the source box.

As a precaution against explosion due to possible contamination of the alcohol through air leaks and contact of the vapor air mixture with the hot wire source, two optical level manometers were mounted on the instrument. One indicated the source box pressure and the other the grating box pressure to within approximately 10^{-3} mm of mercury. In this way leaks in either chamber could be detected quickly before a run was made. The manometers, also, provided a check on vacuum conditions throughout a run.

To obtain some information of the explosion threshold for methyl alcohol, a small explosion flask was designed. This was a vacuum-tight glass container which had a hot wire source sealed into it. Alcohol was introduced in small amounts up to 2 cm of mercury. For a given quantity of alcohol, air was introduced in varying amounts. Each time this was done the wire was heated. Although the control of the amount of vapor and air used in this experiment was not as perfect as one would like it to be, the fact that no ignition took place indicated that the explosion threshold was very likely below two centimeters of mercury pressure, no matter how much air was present.

The amount of vapor pressure introduced into the chamber in this work varied from 2 mm to 16 mm of mercury. The path length was about twelve feet.

After the completion of our experimental work a new spectrometer for the far infrared was constructed at the Ohio State University and Professor R. Oetjen and Dr. E. Palik very kindly offered to run that portion of the methanol spectrum where the lines are most crowded together, namely from 100 to 350 cm^{-1}. Their results were of great value to us in making some of the more difficult identifications and we wish to express our appreciation for their help.

Figures 11 and 12 show the result of combining into a single curve the average of the various runs made by us, by Oetjen and Palik and, at the short wavelength end, by Borden and Barker (*1*). The experimental error in the determination of lines is of the order of 0.2 cm^{-1} although for individual sharp lines it may be as small as 0.1 cm^{-1}. Relative intensities of neighboring lines should be reasonably correct although the accidental piling up of weak background lines may introduce falsifications. The intensities of lines in more widely separated regions of the spectrum have less significance due to the fact that various gas pressures of methanol were employed.

3. METHOD OF ANALYSIS

The first step consists in the calculation of the rotational energy levels neglecting centrifugal distortion, that is, under the assumption that the hydroxyl and methyl groups are individually rigid structures. It is further assumed that the

hydroxyl group may rotate about the symmetry axis of the methyl group subject to a hindering potential $\frac{1}{2}H(1 - \cos 3x)$. Here $x = \phi_1 - \phi_2$ and is equal to the relative rotation angle between the two groups. ϕ_1 and ϕ_2 are the azimuthal angles specifying respectively the rotations of the hydroxyl and methyl groups about the symmetry axis of the molecule. H is the height of the hindering potential. In Ref. *5* the matrix elements of the Hamiltonian are calculated, using as a basis wave functions which would be appropriate for a model in which both the hydroxyl and methyl groups are taken to have coinciding axes of inertial symmetry, that is, both groups may be represented by symmetrical tops having a common axis. These wave functions have the form

$$\mu = (\tfrac{1}{2}\pi)e^{iK\phi}e^{iM\psi}\Theta_{JKM}(\theta)\, M(x),$$

where θ, ϕ, and ψ are Eulerian angles with $\phi = C_1\phi_1/C + C_2\phi_2/C$. The quantity $e^{iK\phi}e^{iM\psi}\Theta_{JKM}$ is the usual symmetric top wave function and describes the overall or external rotation of both of the groups forming the molecule. $M(x)$ relates to the internal or hindered rotation and is equal to $\exp(-iC_1Kx/C)P^{n}_{(x)}{}^{\tau K}$, where

$$P^{n}_{(x)}{}^{\tau K} = \sum_{\rho=-\infty}^{\infty} a_\rho e^{i(3\rho+1-\tau)x}.$$

While it is true that the methyl group may be represented by a symmetrical top, the hydroxyl group is asymmetric and, relative to the symmetry axis of the methyl group, will possess a product of inertia differing from zero. Since the basis wave functions are therefore not energy eigenfunctions, the Hamiltonian matrix of Ref. *5* contains both diagonal and nondiagonal elements, the latter depending upon the asymmetry. The energy levels can be found in the usual manner by solving the energy determinant (diagonalizing the Hamiltonian). In methanol the asymmetry of the hydroxyl group is slight and consequently the nondiagonal elements are small and it will be shown later that, for the most part, they can be ignored.

The diagonal elements of the Hamiltonian may be divided into the sum of three terms. The first of these corresponds to the rotation of the entire molecule and is given by the expression

$$E_{JK} = \hbar^2[(AC_1 + BC_1 - D^2)(J^2 + J - K^2)/4A(BC_1 - D^2) + K^2/2C].$$

A, B, C, C_1, and D are the moments and products of inertia defined in Ref. *5* while J and K are the quantum numbers describing the total angular momentum and its component along the symmetry axis of the methyl group. An evaluation of these constants is made in Ref. *6* by means of the experimentally observed microwave spectrum. The result for methanol expressed in waves per centimeter is,

$$E_{JK}/hc = 0.8066(J^2 + J - K^2) + 4.2544K^2.$$

The second term in the diagonal elements, $E_{n\tau K}$, denotes the internal or hindered rotation energy. This may be calculated by the methods described in Ref. *2* and depends upon the moments of inertia C_1 and C and upon H the height of the potential barrier. The microwave spectrum when analyzed yielded (*6*) $C_1 = 1.245 \times 10^{-40}$ g cm^2, $C = 6.578 \times 10^{-40}$ and $H = 374.82$ cm^{-1}. Using these constants $E_{n\tau K}$ together with the associated Fourier coefficients a_ρ giving the internal rotational wave function $M(x)$, have been calculated for $K = 0$ through 10 and for $n = 0$, 1, 2, and 3. A somewhat condensed table of the a_ρ is given in the Appendix. The internal rotation energy levels through $n = 2$ are plotted in Fig. 1 where the hindering potential is also shown to scale as a dotted curve. The quantum number τ may assume the values 1, 2, or 3 and is

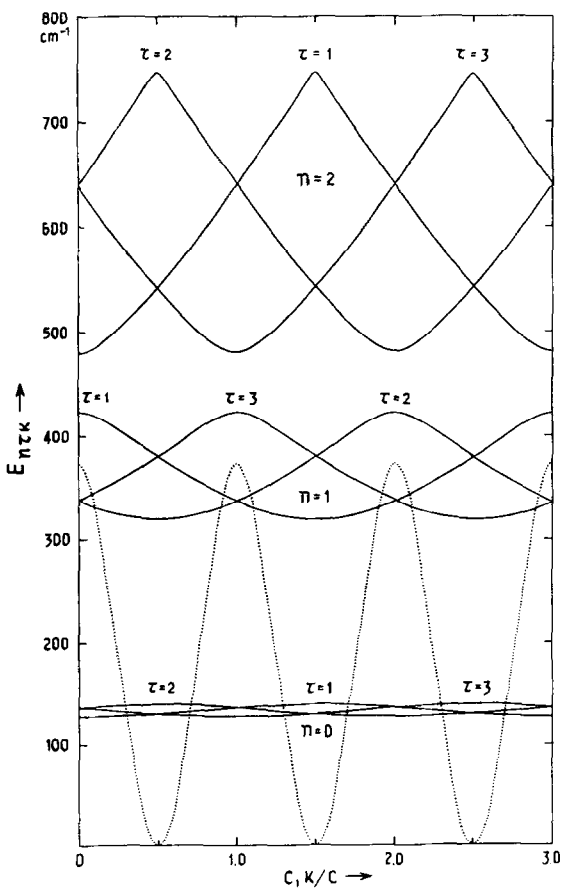

FIG. 1. Internal rotation levels of methyl alcohol

intimately connected with the tunnelling process through which the hydroxyl group may penetrate the three equal barriers presented by the three hydrogens of the methyl group. The $E_{n\tau K}$ are grouped according to the quantum number n. For levels far below the barrier height, n corresponds to the vibrational quantum number in one of the potential minima. For any given τ, $E_{n\tau K}$ is periodic in σK were $\sigma = C_1/C = 0.189275$ for methanol.

From Fig. 1 it will be noted that the levels of $n = 0$ lie far below the potential barrier and consequently the tunnelling frequency is low. The maximum splitting between the various levels is only about 10 cm^{-1}. The splitting is much larger for $n = 1$ while the $n = 2$ levels lie above the barrier and may be reasonably well approximated by a free rotation of the hydroxyl relative to the methyl group.

The third and last of the terms in the diagonal elements of the Hamiltonian arises from the asymmetry of the hydroxyl group. It is equal to $\hbar^2D^2/2C_1(BC_1 - D^2)$ times an integral involving the hindered rotation part of the wave function. Substituting the values of moments and product of inertia for methanol one obtains that the first factor expressed in waves per centimeter is 0.006 cm^{-1}. The second factor may be calculated from the wave functions. It is found to be quite small for most of the levels to be considered and has its greatest value of about 50 for certain of the $n = 3$ levels. The maximum contribution of the term is therefore 0.3 cm^{-1}. Both this term as well as the contributions from the off-diagonal terms will be neglected for the present but will be reexamined somewhat later.

The selection rules for radiative transitions between rotational levels are known (*2*) and have the following form.

(a) For the component of the permanent electric moment lying along the symmetry axis, $\Delta J = \pm 1, 0$, $\Delta K = 0$, $\Delta n = 0$, and $\tau \rightarrow \tau$. These transitions give rise to the series of lines $\nu = hJ(AC_1 + BC_1 - D^2)/8\pi^2A(BC_1 - D^2)$ or using the methanol constants $\nu/c = 1.61J$. The intensities of these lines closely follow the rules for those of a symmetrical rotator and at room temperature the intensity maximum occurs for $J = 20$ where $\nu/c = 32.3$ cm^{-1}. At the beginning of the present experimental range, namely 50 cm^{-1}, their intensity has markedly fallen off and at shorter wavelengths they become negligible in comparison with the Q branch lines about to be described. Hence although they are plotted in Fig. 11 no unique identifications with experimental lines have been possible.

(b) For the component of electric moment of the hydroxyl group perpendicular to the symmetry axis, $\Delta J = \pm 1, 0$ and $\Delta K = \pm 1$. For the transitions where $K \rightarrow K - 1$, τ goes from $1 \rightarrow 2$, $2 \rightarrow 3$, or $3 \rightarrow 1$, while if $K \rightarrow K + 1$, τ goes $2 \rightarrow 1$, $3 \rightarrow 2$, or $1 \rightarrow 3$. Δn may have any value.

Consider a transition $J'', n'', \tau'', K \rightarrow J', n', \tau', K - 1$. The frequencies, using

the expressions for the external and internal energies of methanol already given and remembering that $J \geqslant K$, may be written,

$$(\nu/c)_{J\to J-1} = \nu'/c + 1.6132J \qquad J = K, K+1, K+2, \cdots,$$
$$(\nu/c)_{J\to J} = \nu'/c$$
$$(\nu/c)_{J-1\to J} = \nu'/c - 1.6132J \qquad J = K+1, K+2, \cdots,$$

where

$$\nu'/c = (3.4478)(2K-1) + (E_{n''\tau''K} - E_{n'\tau'K-1})/hc.$$

These lines may be said to form a sub band of P, Q, and R branches with Q branch at ν'/c. The other possible transition in which $K - 1 \to K$ will of course have a similar structure.

The spacing of the lines in the P and R branches is constant and for methanol has the approximate value of 1.6 cm^{-1}. The relative intensities within a given sub band are equal to those in any sub band associated with a perpendicular vibration of a symmetrical rotator. As is well known (*10*) the integrated intensity of the Q branch, which is composed of many superimposed lines, is approximately equal to the sum of the intensities of all the lines of the P and R branches. This fact gives the key to the general appearance of the spectrum. In those regions where the sub bands fall close to each other—and this is the situation for most of the spectrum—the Q branches will stand out as individual lines which by reason of the hindered rotation contributions will be irregularly distributed both in position and intensity. The P and R branch lines associated with these Q branches form an intermingling pattern of background lines which in general will not be resolved, at least with the present spectrometer. However in a region where the sub bands are more widely spaced one may expect to find evidence of the P and R branch lines particularly where by chance the P branch lines of one sub band coincide with the R branch lines of some other sub band. This appears to be the origin of the series of uniformly spaced lines occurring near 560 cm^{-1}, for example, and indeed it is possible to identify the particular sub bands responsible for this series and to verify that they have approximately the predicted intensity distribution. For the most part, however, the sub bands are so crowded together that it is not possible to identify or even to observe the individual P and R lines. Consequently in what follows they will be ignored and attention will be paid exclusively to the Q branch lines.

The intensities of the Q branches are to be found through the usual procedure of calculating the matrix elements of the electric moment and combining these with the distribution of the molecules in the various energy states. Just as the wave function may be divided into factors describing a symmetrical rotator and a hindered rotator, so also the resulting intensity may be similarly divided. It

will be convenient to use the following expression for the intensity of the Q branch resulting from a transition from the lower energy state E' to a higher state E''.

$$I_{E'\to E''} = A\nu f_{\tau' K'} F_{K' K''}(n'\tau' K' \mid \mathfrak{M} \mid n''\tau'' K'')^2(1 - e^{-h\nu/kT}) \exp(-E'_{n\tau K}/kT.)$$

In this formula A is a constant, ν the frequency of the line, and $f_{\tau' K'}$ is a weight factor arising from spins of the protons in the methyl group which must of course obey Fermi-Dirac statistics. As in other molecules having threefold symmetry (for example, the methyl halides) one third of the states have an enhancement factor of 2. Using the symmetry species of the states described by Ivash and Dennison (*6*), it is readily shown that $f_{\tau K} = 2$ for $\tau = 1$, $K = 0, 3, 6, \cdots$ for $\tau = 2$, $K = 2, 5, 8, \cdots$ and for $\tau = 3$, $K = 1, 4, 7, \cdots$ while for all other values $f_{\tau K} = 1$.

$F_{K' K''}$ is the intensity of a Q branch for a symmetrical rotator where the transition is one where $K' \to K''$ and $J \to J$. K'' must of course be equal to $K' \pm 1$ and J is equal to or greater than K' or K'' whichever is the larger. $F_{K' K''}$ contains the square of the matrix element associated with the transition, the number of molecules in the initial state and finally a sum over all values of J. In the case of methyl alcohol at room temperature the difference in the energy levels occurring in the sum is small compared with kT, the thermal energy, and consequently the sum may be replaced by an integral as was done by Gerhard and Dennison (*10*) in calculating the envelopes of symmetrical top bands. The final formula is,

$$F_{K,K\pm 1} = e^{-\sigma\beta K^2}[e^{-\sigma K^2} + \sigma K^2 \int_{\infty}^{\sigma K^2} \frac{e^{-u}}{u}\, du,$$

where $\sigma = \hbar^2/2AkT = 0.00387$ at room temperature and $\beta = C/A - 1 = 4.37$.

The factor $(1 - e^{-h\nu/kT})$ takes care of the effect of the induced inverse transitions. Although it has been included in the present calculation, clearly it has little significance in identifying the lines since it can not affect the relative intensities of neighbors. $E'_{n\tau K}$ is the internal or hindered rotation energy of the lower state. The portion of the Boltzmann factor depending upon the external or overall rotation has been taken account of in $F_{K' K''}$. $(n'\tau' K' \mid \mathfrak{M} \mid n''\tau'' K'')$ is that contribution to the matrix element of the electric moment coming from the internal rotation wave function $M(x)$ as shown in Ref. *2*, p. 1016, and is equal to

$$\sum_{-\infty}^{+\infty} a_\rho' a''_{\rho-1} \quad \text{for} \quad K \to K - 1 \quad \text{or to} \quad \sum_{-\infty}^{+\infty} a_\rho' a''_{\rho+1} \quad \text{for} \quad K \to K + 1.$$

Using the Fourier coefficients a_ρ already evaluated for methanol $(n'\tau' K' \mid \mathfrak{M} \mid n''\tau'' K'')$ has been calculated and its absolute value is plotted in Figs. 2 through

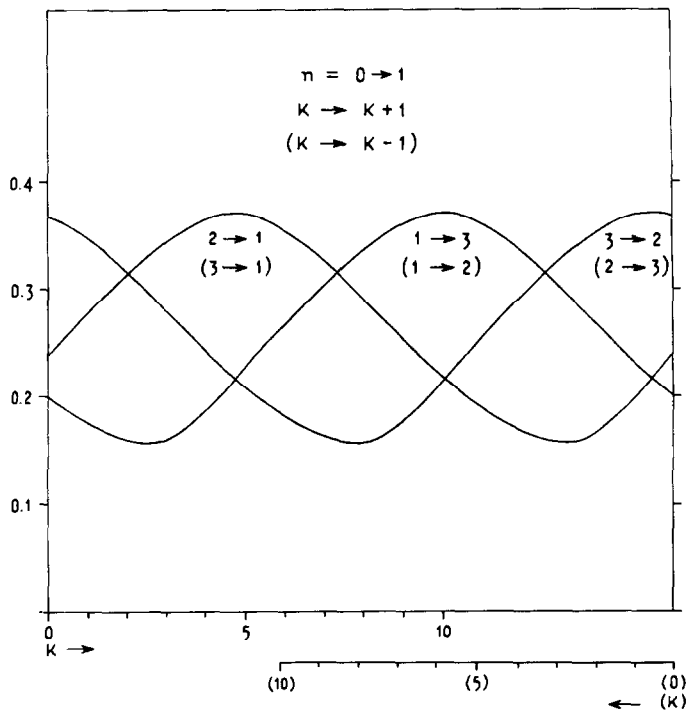

FIG. 2. Internal rotation intensity factor, $n = 0 \rightarrow 1$

10 for the various values of n' and n'' which might give rise to lines in the observed region of the spectrum. The curves for $n = 0 \rightarrow 0$ have been omitted since they are virtually straight horizontal lines of height unity.

In these figures the two possibilities $K \rightarrow K + 1$ and $K \rightarrow K - 1$ are differentiated by bracketing the labels for the latter transitions. It will be noted that the K scale goes from left to right for the $K \rightarrow K + 1$ transitions and from right to left for the $K \rightarrow K - 1$. For example in the transition $n = 0 \rightarrow 2$ and $K = 3 \rightarrow 4$, $|\mathfrak{M}|$ for $\tau = 2 \rightarrow 1$, $3 \rightarrow 2$, and $1 \rightarrow 3$ has the respective values 0.010, 0.053 and 0.109. If $K = 3 \rightarrow 2$ however $\tau = 1 \rightarrow 2$, $2 \rightarrow 3$, and $3 \rightarrow 1$ and the corresponding values of $|\mathfrak{M}|$ are 0.046, 0.011 and 0.105.

At this point the energy levels as calculated from the molecular constants as well as expressions giving the intensities of the lines are available. An attempt was made to compare the calculated and observed lines for the transitions belonging to $n = 0 \rightarrow 2$. The reason for selecting these transitions was that the resulting lines fall, for the most part, between 350 and 600 cm^{-1}. Here the density of lines is much smaller than it is in the longer wavelength region and consequently there is a greater certainty of making unambiguous identifications.

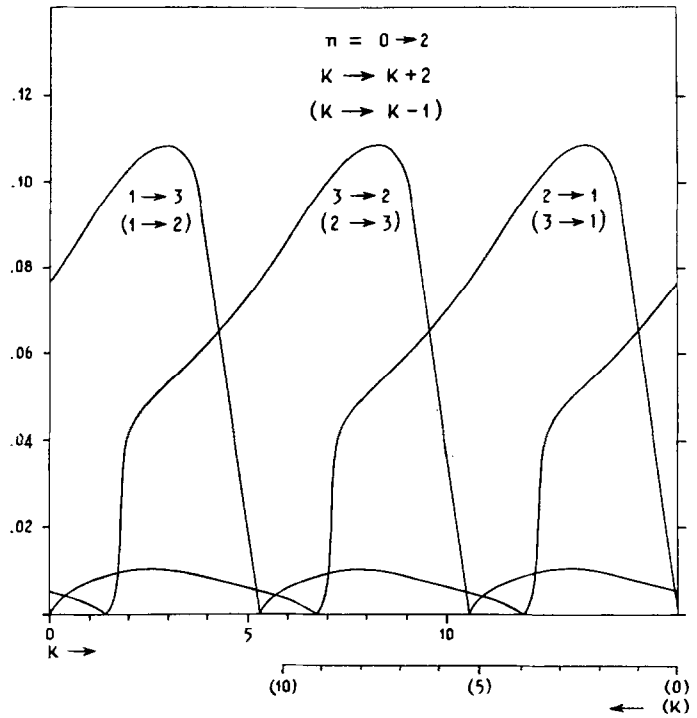

FIG. 3. Internal rotation intensity factor, $n = 0 \rightarrow 2$

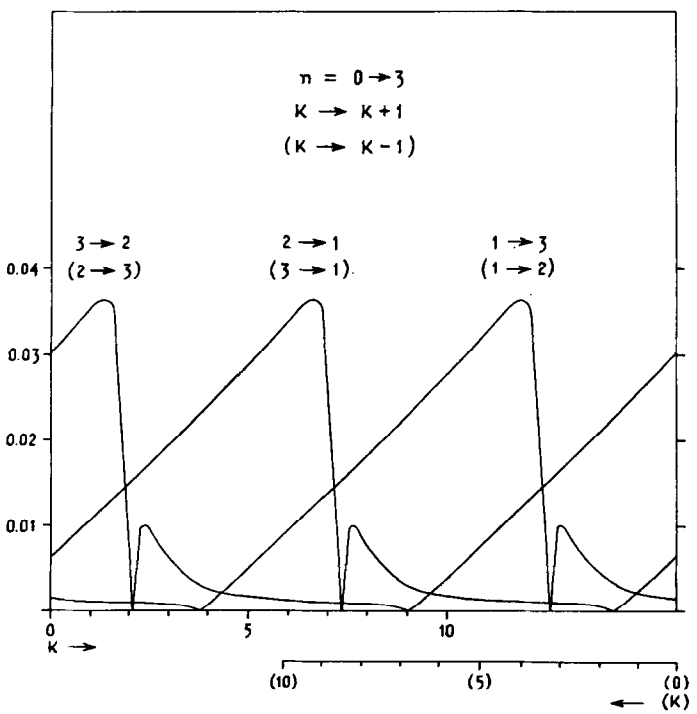

FIG. 4. Internal rotation intensity factor, $n = 0 \rightarrow 3$

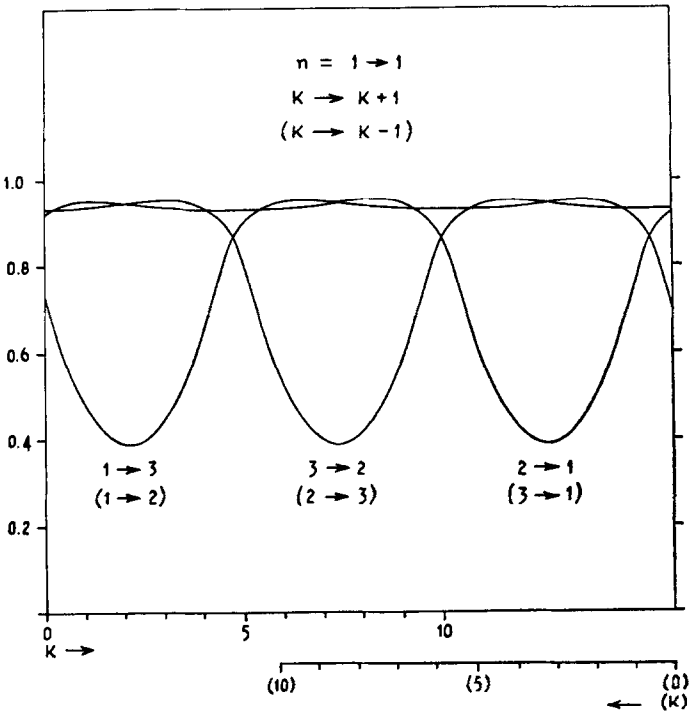

FIG. 5. Internal rotation intensity factor, $n = 1 \rightarrow 1$

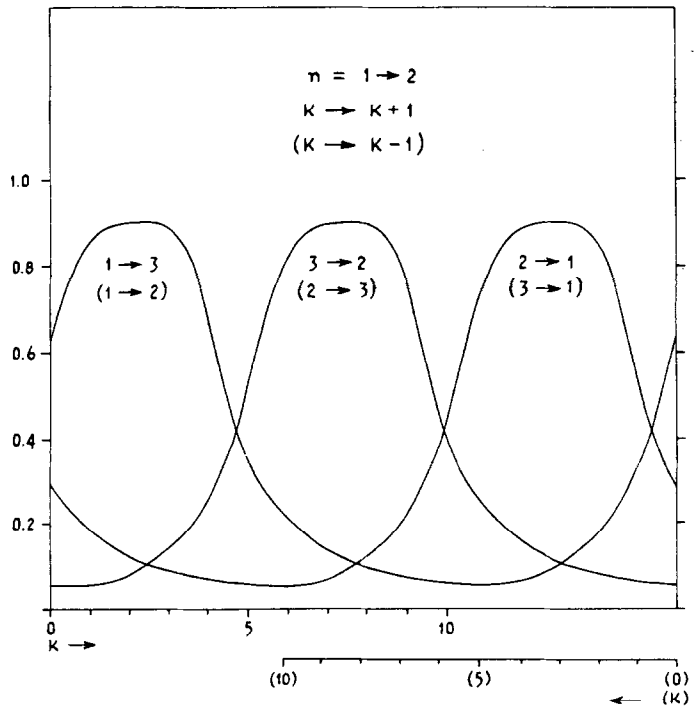

FIG. 6. Internal rotation intensity factor, $n = 1 \rightarrow 2$

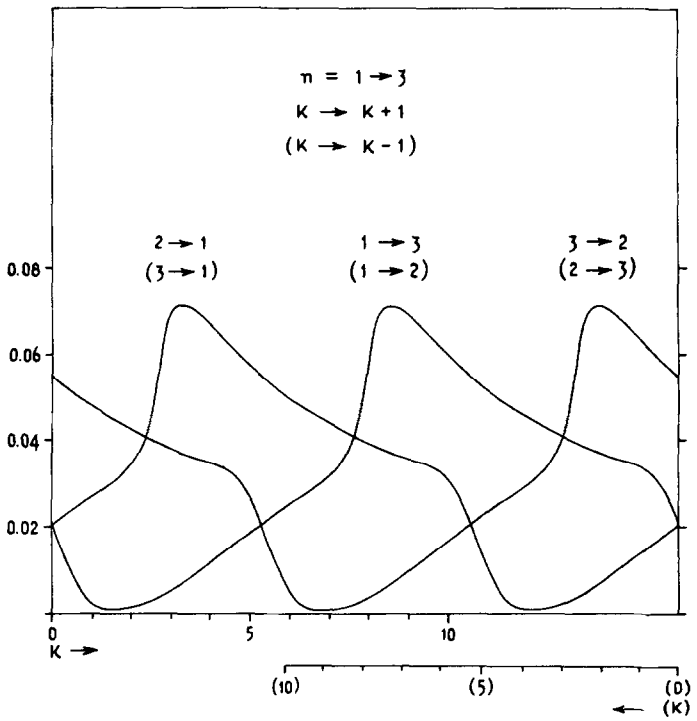

FIG. 7. Internal rotation intensity factor, $n = 1 \rightarrow 3$

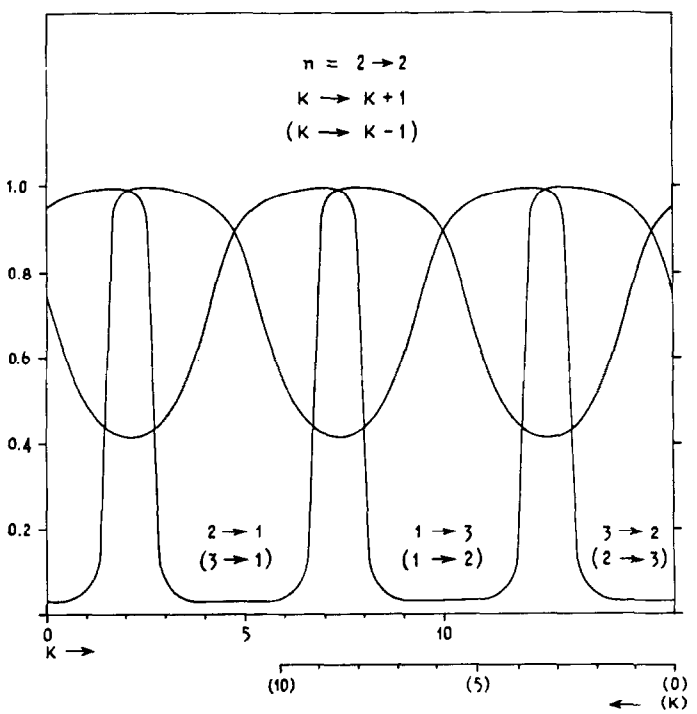

FIG. 8. Internal rotation intensity factor, $n = 2 \rightarrow 2$

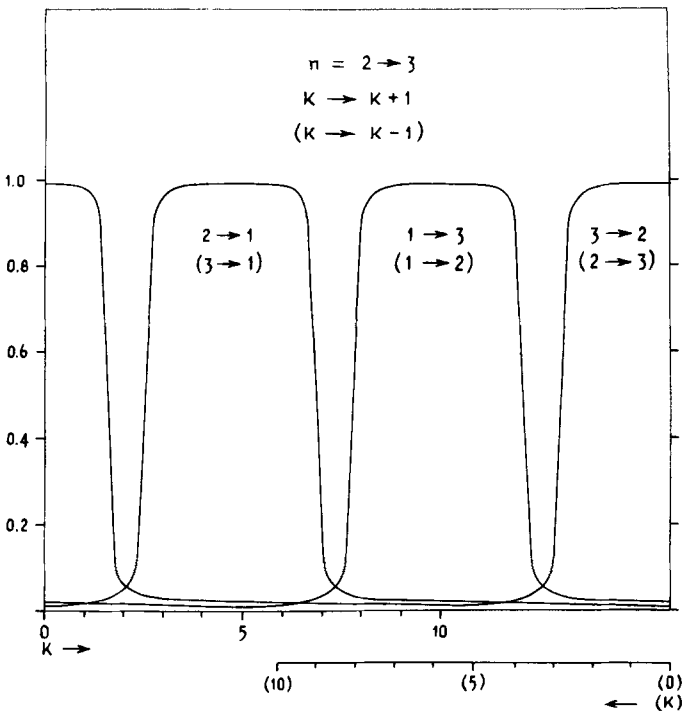

FIG. 9. Internal rotation intensity factor, $n = 2 \rightarrow 3$

A study of this portion of the calculated and observed spectrum showed that it was indeed possible to identify most of the lines but that the calculated lines were shifted from the observed ones by amounts varying up to as much as 10 or 12 cm^{-1}. The magnitudes of the shifts for any particular τ transition, say $K \rightarrow K - 1$, $\tau = 1 \rightarrow 2$ were found to depend in a regular fashion upon K but this dependence varied for the different τ transitions. From the direction and order of magnitude of the shifts it seemed probable that they must be due to centrifugal distortions and an attempt was made to estimate the magnitude of the effect. It may be helpful to present the calculation initially from a semiclassical viewpoint and later to give the formulas arising from a quantum theory treatment.

The levels of $n = 2$ in methyl alcohol lie well above the potential barrier and consequently may be approximated with very fair accuracy by a model where the methyl and hydroxyl groups perform free rotations with respect to each other. The free rotation case has been studied by Koehler and Dennison (*2*) and the energies and wave functions may be described by the quantum numbers J, K and m representing respectively the total angular momentum, the com-

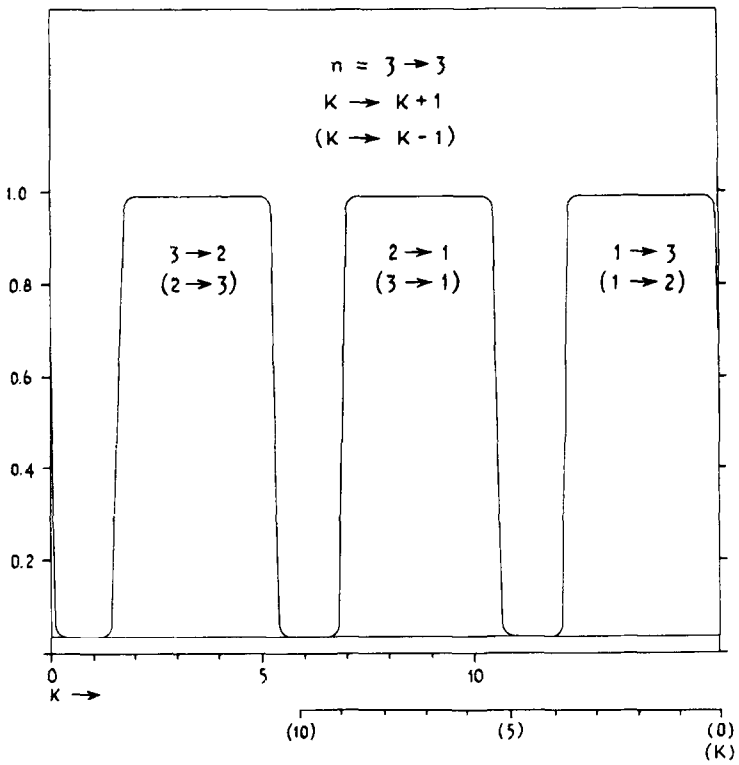

FIG. 10. Internal rotation intensity factor, $n = 3 \rightarrow 3$

ponent of total angular momentum along the symmetry axis and the axial component of the angular momentum due to the hydroxyl group alone. The energy has the expected form

$$E = (J^2 + J - K^2)\hbar^2/2A + m^2\hbar^2/2C_1 + (K - m)^2\hbar^2/2C_2 .$$

Koehler and Dennison show that a given level may be described either by the numbers J, K, m appropriate for the free rotation, or by the numbers J, K, τ, n appropriate for the hindered rotator, and rules are given for obtaining one set of numbers from the other set.

The centrifugal distortion contributions to the energy will be, as usual, quartic in the angular momenta and, in fact, depend upon the quadratic combinations of $(J^2 + J)$, m^2, and $(K - m)^2$. The rotational frequencies (classically speaking for the moment) corresponding to the rotations of either the hydroxyl or the methyl groups about the symmetry axis are much higher than precessional frequency associated with J. This of course arises from the fact that the moment

of inertia A is very much larger than either C_1 or C_2. Since the centrifugal distortion contributions are quartic in the frequencies, it follows that the terms involving $(J^2 + J)$ are much smaller than those containing only K or m. A reasonable estimate of the centrifugal effect may be made therefore by choosing any particular value of J. The work will be made much simpler by letting $J = K$ since this means that the motion consists only of rotations about the symmetry axis.

Consider first the centrifugal distortion caused by the rotation of the hydroxyl group. The change in energy is quartic in m and a standard calculation shows it to be

$$\Delta E_1 = -\sum_i (\hbar^4/8k_i)(C^1_{1i}/C^1_{10})^2 m^4,$$

where k_i is the elastic force constant associated with the ith normal vibration and is equal to $4\pi^2\mu_i\nu_i^2$ where μ_i is the reduced mass associated with this vibration. C_{10} is the equilibrium value of the moment of inertia of the hydroxyl group and $C^{(1)}_{1i}$ is the derivative of C_1 with respect to the ith normal coordinate, $C^{(1)}_{1i} = (\partial C_1/\partial q_i)_0$. These terms have already been evaluated by Hecht and Dennison (*11*) using valence coordinates as an approximation of normal coordinates. The deformation of the HOC angle and the stretching of the OH distance give contributions 4.2×10^{-3} cm^{-1} and 2.9×10^{-3} cm^{-1}, respectively.

The change in energy due to the centrifugal distortion of the methyl group is given by a similar formula and is proportional to the fourth power of the angular momentum of that group, namely $\hbar(m - K)$. The coefficient of $(m - K)^4$ might be evaluated through the elastic force constants of the methyl group. At this point however we are mainly interested in its approximate value and we shall use the value calculated by Chang (*12*)[1] for methyl chloride, namely 0.86×10^{-4} cm^{-1}. The classical treatment of the centrifugal distortion terms has therefore yielded,

$$\Delta E/hc = -7.1 \times 10^{-3} m^4 - 0.86 \times 10^{-4}(m - K)^4.$$

A substitution of the appropriate values of m and $m - K$ for the levels of $n = 2$ (where m is a relatively good quantum number) markedly closed the gaps between the calculated and observed positions of the lines $n = 0 \rightarrow 2$ although it was clear that further adjustments would be necessary to obtain exact agreement.

The problem of the centrifugal distortion effects was now reexamined using the quantum mechanical treatment employed by Hecht and Dennison (*11*). The results were as follows.

(1) The dominant terms are identical with those obtained using classical methods except that m^4 and $(m - K)^4$ are to be replaced by their expectation

[1] The quantity in question is $D_{KK} = 2587$ kc/sec $= 0.86 \times 10^{-4}$ cm^{-1}.

values. These are expressable as functions of the Fourier coefficients appearing in the internal rotation wave functions. Thus $\langle m^4 \rangle = \sum \rho^4 a_\rho^2$ and $\langle (m - K)^4 \rangle = \sum (\rho - K)^4 a_\rho^2$.

(2) Terms appear which arise from the change of barrier height with the centrifugal distortion of the molecule. One of these is proportional to the expectation value of m^2, namely $\sum \rho^2 a_\rho^2$, times the diagonal matrix element of the potential energy function $(1 - \cos 3x)$. The interpretation of this term is evident. $\langle m^2 \rangle$ is proportional to the centrifugal force acting upon the hydrogen nucleus of the hydroxyl group and gives rise to a distortion of the molecule whose magnitude depends upon the elastic constants. It is to be expected that such a distortion will raise or lower the barrier height by a small amount and that its influence upon the energy levels will be proportional to the average value of the potential energy function.

The coefficient of $\langle m^2 \rangle \langle 1 - \cos 3x \rangle$ can not be calculated without a much deeper knowledge of the nature of the hindering potential than we now possess. It is however possible to make a very rough estimate of its order of magnitude. Consider those levels which lie above the barrier and which may be approximated by a free rotation. The change in energy will be approximately equal to the change in the average potential caused by the centrifugal distortion, that is, to $\frac{1}{2}\Delta H \langle 1 - \cos 3x \rangle$. For these levels $\langle 1 - \cos 3x \rangle \cong 1$. In rough order of magnitude one could expect that $\Delta H \sim \pm \mid \Delta r/r_0 \mid H \pm \mid \Delta\theta \mid H$ where $\Delta r/r_0$ is the relative change in the OH distance, $\Delta\theta$ the change in the COH angle and H is the height of the potential barrier. By balancing the centrifugal force against the elastic potential forces (the OH and COH potential constants were taken as 7.5×10^5 and 0.62×10^5 dynes/cm, respectively) one readily obtains $(\Delta r/r_0)H = (0.05)\langle m^2 \rangle$ cm^{-1} and $H\Delta\theta = 0.17\langle m^2 \rangle$ cm^{-1}. Thus the coefficient of $\langle m^2 \rangle \langle 1 - \cos 3x \rangle$ could well be of the order of a few tenths of a wave per centimeter but clearly neither its true magnitude nor even its sign can be calculated with any certainty.

In addition to the term just discussed there are further terms which may be associated with the dependence of barrier height on the normal coordinates. Most of these are small but there is one which might produce significant effects and which is proportional to the expectation value of $(1 - \cos 3x)^2$. It would be very difficult however to disentangle this term from the effects of a first order correction to the assumed sinusoidal potential, namely $\langle (1 - \cos 6x) \rangle$. A discussion of such corrections will be given later.

Two additional remarks must be made before proceeding with the identification of the spectral lines and hence the determination of the rotational levels of the molecule. The first of these relates to the fact that the Q branch lines, on which attention is to be focused, are of course multiple lines since each consists of a superposition of all the $J \rightarrow J$ transitions where $J \geqslant K$. The usual interac-

tion between vibration and rotation will separate the components and produce a convergence which is proportional to $J^2 + J$. The proportionality factor will depend upon the rotational state (including internal rotation) and its sign may be expected to change as K increases or decreases. The spectrometer used in the present investigation will not resolve the components but it does often reveal an asymmetry of the line. The recorded maximum will thus be shifted by this convergence from its calculated position. In the following discussion the convergence of the Q branch components will be ignored and this will lead to two results. In the first place, the values of the rotational levels as determined from the observed lines will not be correct to better than the magnitude of the convergences. These may be estimated to be of the order of a few tenths of a wave per centimeter. Secondly, combination relations will fail to be satisfied by the same amounts. This will be particularly true when the lines in question correspond to K transitions, some of which increase and some decrease. For these reasons no attempt will be made to fix the energy levels with an accuracy greater than a few tenths of a wave per centimeter and all corrections smaller than this will be ignored.

The second remark concerns the effect of the asymmetry of the molecule on the positions of the levels. There is the diagonal element

$$-[\hbar^2 D^2/2C_1(BC_1 - D^2)] \int (P^{n\tau K})^* \frac{d^2}{dx^2} P^{n\tau K}\, dx$$

mentioned earlier. A substitution of the methanol constants showed that the contribution of the term is usually very small but might be as large as 0.3 cm^{-1} for certain of the $n = 3$ levels.

The zeroth order Hamiltonian also contains off-diagonal terms connecting the states K with $K \pm 1$ and $K \pm 2$. When the energy matrix is diagonalized these furnish contributions which are approximately proportional to $J^2 + J$ and to $(J^2 + J)^2$. The coefficients of these quantities were given by Burkhard and Dennison (*5*) for a particular transition and found to be around 5×10^{-5} cm^{-1} and 3×10^{-6} cm^{-1}, respectively. An inspection of the elements shows that they differ for the various levels since they contain integrals over the hindered rotation wave functions. These integrals however are of the order of magnitude of unity and consequently the above figures are reasonably representative of the expected size of these terms. The population of states in its J dependence is proportional to $(2J + 1) \exp[-\sigma(J^2 + J)]$ where $\sigma = 0.00387$ for methanol at room temperature. The population increases with J, reaches a maximum at $J \cong 11$ and subsequently declines sharply. The effect of these off-diagonal elements of the Hamiltonian will therefore be to spread out the lines over a region of the order (using $J = 0$ to 20) of around 0.5 cm^{-1}. It will form part of the convergence of the Q branch lines already discussed and since its precise magnitude varies from

line to line it will contribute to deviations of the energy levels and of the combination relations in the amount of a few tenths of a wave per centimeter.

The final effect of the asymmetry which will be discussed is the K-type doubling described by Ivash and Dennison (*6*). They have shown that for every K (except $K = 0$) one of the three levels corresponding to the three τ numbers is split into a doublet. The magnitude of the splitting depends upon J and K. It falls off rapidly with K however and the principal hope of observing it in the infrared spectrum will occur for the levels where $K = 1$. The split level is here the one where $\tau = 3$. Ivash and Dennison give as the splitting formula,

$$\Delta E = 2H^{J,1}_{J,-1}$$

$$= (J^2 + J)[\hbar^2(C_1^2 + D^2)/4A(BC_1 - D^2)] \int (P^{n,2,-1})^* e^{-2ix} P^{n,3,1}\, dx.$$

The integral may be calculated through the use of the Fourier coefficients which describe the hindered rotation wave functions. By this means one obtains the following expressions for the splitting of the levels (031), (131), and (231), respectively [here as in the remainder of the paper a level will be designated by the symbol $(n\tau K)$].

$$\Delta E/hc = 0.013(J^2 + J),$$

$$\Delta E/hc = 0.0016(J^2 + J),$$

$$\Delta E/hc = 0.0028(J^2 + J).$$

Clearly transitions involving (031) will show the largest effects. These are $(n10) \rightarrow (031)$ and $(n22) \rightarrow (031)$. The selection rules (see Ref. *6*) are such that the first of these transitions will contain only one member of the doublet, and therefore the net effect will be to shift the position of the line. The second transition will however consist of a doublet, each component of which is made up of individual lines corresponding to the different values of J. The intensities of these lines, in their J dependency, will be proportional to

$$[(2J + 1)(J - K + 1)(J + K)/J(J + 1)]e^{-\sigma(J^2+J)}.$$

For the transition in question $K = 2$ and for all except the lowest J values, the intensity is roughly proportional to $(2J + 1)\exp[-\sigma(J^2 + J)]$. The line of maximum intensity is again that for which $J \cong 11$. The doublet, that is, the distance between the two most intense lines, is 1.7 cm^{-1}. The spacing between the lines is roughly $0.013J$ cm^{-1} which, for low J, is considerably below the limit of resolution of the spectrometers used in the experiment. Consequently the observed intensity when the spectrometer slit, which will include a number of lines, is centered at the Jth line should be porportional to $[(2J + 1)/J]\exp$

$[-\sigma(J^2 + J)]$ and therefore we will not expect to see a doublet but only a single broadened line whose half width may be calculated from the above data to be 2.3 cm^{-1}. The corresponding lines $(n22)$–(131) and $(n22)$–(231) should have half widths of 0.3 and 0.5 cm^{-1}, respectively.

An examination was made of all the lines assigned to transitions involving the states (031), (131), and (231). Some of these appear to be rather wide but on the whole they are indistinguishable from the other spectral lines. As the most extreme example we might cite the following. The level (122) is well established through the strong line (122)–(013) = 172.7 cm^{-1}. This leads to the prediction that (122)–(031) should lie close to 197.2 cm^{-1}. Experimentally, there is a line at 197.7 cm^{-1} which would fit reasonably well and which is of about the right intensity although it is somewhat weaker than expected. This line is in no way unusual in appearance and has a half width which is certainly much less than the predicted value of 2.3 cm^{-1}. One possible explanation is that the line observed at 197.7 cm^{-1} is due to some other cause and that (122)–(031) is sufficiently broad so that it merges into the ever present background of P and R branch lines and hence is undetected. The situation is puzzling and it is hoped that further experimental work may resolve the apparent discrepancies.

4. EVALUATION OF THE ENERGY LEVELS

The following procedure was employed. (a) The unperturbed energy levels were calculated for the states $n = 0, 1, 2, 3$ and for $K = 0$ through 10 using the barrier height and moments of inertia determined by Ivash and Dennison. (b) All the transitions allowed by the selection rules were listed and their intensities calculated. In both of these computations effects due to the asymmetry of the molecules were ignored since it has been shown that they may be expected to be small. (c) A comparison was made between the most intense lines of the

$$n = 0 \rightarrow 2$$

transitions of the calculated and the observed spectrum. As explained earlier, these lines fall in a relatively clear region of the spectrum and a unique identification was possible. (d) A centrifugal distortion correction to the calculated levels was made which had the form $a\langle m^4\rangle + b\langle (m - k)^4\rangle + c\langle m^2\rangle\langle 1 - \cos 3x\rangle$. The coefficients a, b, c were adjusted to give a fit between the calculated and observed lines of the $n = 0 \rightarrow 2$ transitions.

A number of sets of coefficients were found each of which gave substantially equally satisfactory agreements between the calculated and observed lines. The differences in a particular coefficient between the different sets were of the order of 20% where in general an increase in the coefficient a was compensated by a decrease in c. The following values were adopted. These are seen to be of the orders of magnitude predicted earlier. $a = -0.0063$ cm^{-1}, $b = -0.0003$ cm^{-1},

$c = -0.14$ cm^{-1}. (e) The next step of the procedure consisted in evaluating the corrections described above for all levels and thus obtaining revised spectral lines which could be compared with the observed lines. In most cases it was possible on the basis of both the positions and intensities to make unique identifications. Once the identifications were made it was of course easy to obtain the energy levels providing one possessed the base levels from which to start. Since the energy corrections [as given under step (d)] were quite small for the levels of $n = 0$ and $K = 0$ to 10, these were taken to be correct and the levels of $n = 1, 2, 3$ were found as the sum of one or more observed lines and one of the calculated $n = 0$ levels. In what follows, these will be called observed levels. It would be more satisfactory of course if transitions between the $n = 0$ levels themselves could be identified. Unfortunately this has not been possible up until now since the lines in question lie between 0 to 70 cm^{-1}, and thus for the most part fall outside our experimental region.

The final results of this procedure are presented in Tables I through IV for the values of $n = 0$, 1, 2, and 3. In each table the levels are listed as a function of their kind, namely $\tau = 1$, 2, or 3 and for $K = 0$ to 10. The first column, $-\Delta E$, gives the calculated centrifugal distortion energy corrections [described in step (d)]. Here, as in the remainder of the table, it is convenient to give the quantities in units of waves per centimeter. The proper label for the column therefore would be $-\Delta E/hc$.

The second column, $E_{\text{calc.}}$, gives the calculated energies in cm^{-1} and includes (1) the external rotational energy which is equal to $3.4478K^2$, (2) the internal or hindered rotational energy, $E_{n\tau K}$, and (3) the centrifugal correction $-\Delta E$.

Table I.

Levels of n = 0

	τ = 1		τ = 2		τ = 3	
K	- ΔE	$E_{calc.}$	- ΔE	$E_{calc.}$	- ΔE	$E_{calc.}$
0	0.2	128.6	0.2	137.7	0.2	137.7
1	0.2	132.5	0.2	143.2	0.2	138.7
2	0.2	144.1	0.3	154.8	0.2	146.6
3	0.3	163.2	0.3	172.2	0.3	161.8
4	0.4	189.6	0.4	195.2	0.3	184.4
5	0.5	223.0	0.5	224.3	0.4	214.7
6	0.7	263.0	0.7	259.7	0.6	252.6
7	0.9	309.1	0.9	301.8	0.8	298.2
8	1.3	360.9	1.2	351.1	1.2	351.3
9	1.8	418.4	1.5	407.7	1.7	411.7
10	2.4	481.7	2.0	471.8	2.4	479.1
11	3.0	551.2	2.7	543.5	3.4	552.8

Table II.

Levels of n = 1

	τ = 1			τ = 2			τ = 3		
K	- ΔE	$E_{calc.}$	$E_{obs.}$	- ΔE	$E_{calc.}$	$E_{obs.}$	- ΔE	$E_{calc.}$	$E_{obs.}$
0	1.8	423.6	423.7	0.9	337.9	337.5	0.9	337.9	337.5
1	1.9	416.3	416.3	0.9	331.6	331.1	0.9	355.0	354.3
2	1.9	406.7	406.4	0.8	336.6	336.1	1.0	382.3	381.9
3	1.9	404.0	403.7	0.8	353.1	352.6	1.2	418.9	418.5
4	1.9	410.3	410.1	0.9	381.3	380.9	1.6	463.0	462.7
5	1.9	426.6	426.8	0.9	420.9	420.6	2.2	508.3	507.9
6	1.9	453.6	452.5	1.2	471.2	470.2	3.3	540.2	540.1
7	1.9	491.7	491.2	1.7	531.7	531.8	3.9	565.8	565.6
8	2.1	541.2	541.2	2.4	601.6	601.7	4.1	597.0	597.3
9	2.6	602.1	601.8	3.5	679.5	679.7	4.3	636.9	637.0
10	3.3	674.3	674.3	5.4	760.9	761.7	4.7	686.3	686.6

Table III.

Levels of n = 2

	τ = 1			τ = 2			τ = 3		
K	- ΔE	$E_{calc.}$	$E_{obs.}$	- ΔE	$E_{calc.}$	$E_{obs.}$	- ΔE	$E_{calc.}$	$E_{obs.}$
0	2.1	481.5	481.4	4.2	638.8	638.9	4.2	638.8	638.9
1	2.1	498.2	498.3	4.3	683.8	683.7	4.1	603.0	603.3
2	2.2	535.9	535.8	4.5	737.8	737.8	4.1	576.6	576.9
3	2.3	585.7	585.7	7.7	764.5	764.2	4.1	560.1	560.3
4	2.6	645.6	645.7	7.7	744.3	744.4	4.0	555.0	555.3
5	3.1	714.7	714.8	7.7	733.1	733.0	3.3	567.8	568.3
6	3.8	793.0	793.2	7.7	731.0	731.1	2.3	612.8	612.9
7	4.8	880.0	880.2	7.8	738.3	738.7	2.7	682.0	682.6
8	12.6	961.3	961.3	7.8	755.3	755.8	3.6	764.5	764.0
9	13.6	975.0	975.0	7.7	783.1	783.9	4.8	857.0	856.9
10	13.6	997.6	997.8	7.2	826.0	826.7	6.6	958.7	959.2

The last column lists the observed energies as found by using the most reliable lines in the observed spectrum. A blank here means that no lines were observed which could fix the level in question. In the case of Table I for $n = 0$ only calculated values for the energy are listed since, as remarked earlier, the present range of the observed infrared spectrum does not include a sufficient number of identifiable $n = 0 \rightarrow 0$ transitions.

In treating a spectrum, such as the rotational spectrum of methanol where the lines are irregularly spaced and where they often crowd together so closely

Table IV.

Levels of n = 3

	τ = 1			τ = 2			τ = 3		
K	$-\Delta E$	$E_{calc.}$	$E_{obs.}$	$-\Delta E$	$E_{calc.}$	$E_{obs.}$	$-\Delta E$	$E_{calc.}$	$E_{obs.}$
0	13.7	1176.5	-	7.9	879.5	879.4	7.9	879.5	879.4
1	13.5	1118.1	-	7.8	832.3	832.3	8.1	935.7	935.6
2	13.5	1069.1	1067.9	7.7	794.0	793.8	8.4	1000.6	-
3	13.4	1028.9	1027.9	4.8	800.7	801.1	8.9	1074.3	-
4	13.4	997.4	997.0	5.3	872.5	-	9.6	1156.9	1156.2
5	13.5	974.9	974.5	6.0	953.4	953.3	10.6	1248.1	-
6	13.5	961.4	961.2	7.0	1042.2	1042.2	22.3	1247.6	1247.3
7	13.5	957.0	-	8.4	1140.0	-	22.4	1232.1	1232.5
8	6.3	981.9	-	10.2	1246.3	1246.3	22.4	1225.6	-
9	8.1	1079.9	1080.0	12.4	1361.3	-	22.4	1228.1	-
10	10.4	1192.8	-	15.5	1484.4	-	22.5	1239.5	-

that they are imperfectly resolved, the difficulty lies in having confidence in the uniqueness of the identifications. Accordingly, a great number of tests were made. In the first place a comparison may be made between the predicted and observed spectrum. Tables V–VIII list the lines corresponding to transitions to the levels $n = 0$, 1, 2, and 3, respectively. The first column gives the label of the line $(n\tau K) - (n'\tau'K')$ and the second column contains the calculated square root intensity, $I^{1/2}$. In most observations of infrared spectra, and certainly in the present case, the width of the individual lines is less than the resolving power of the spectrometer. Under these conditions it is well known that the apparent in-

TABLE V.

Lines From the Levels of n = 0

Line	$I^{1/2}$	ν	δ	Line	$I^{1/2}$	ν	δ	Line	$I^{1/2}$	ν	δ
031-010	1.0	10.1	-	021-030	0.4	5.5	-	020-011	0.3	5.2	-
032-011	0.9	14.1	-	022-031	1.4	16.1	-	012-021	0.16	0.9	-
033-012	1.1	17.7	-	023-032	1.5	25.6	-	013-022	0.7	8.4	-
034-013	1.6	21.2	-	024-033	1.9	33.4	-	014-023	1.0	17.4	-
035-014	1.3	25.1	-	025-034	2.8	39.9	-	015-024	1.3	27.8	-
036-015	1.3	29.6	-	026-035	2.0	45.0	-	016-025	2.4	38.7	-
037-016	1.9	35.2	-	027-036	1.9	49.2	-0.3	017-026	1.9	49.4	-0.1
038-017	1.4	42.2	-	028-037	2.4	52.9	0.0	018-027	1.8	59.1	-0.1
039-018	1.4	50.8	-	029-038	1.5	56.4	0.1	019-028	2.3	67.3	-0.4
0310-019	1.8	60.7	-0.2	0210-039	1.3	60.1	-	0110-029	1.6	74.0	0.3
0311-0110	1.2	71.1	-	0211-0310	1.5	64.4	0.2	0111-1210	1.3	79.4	-

TABLE VI.

Lines From the Levels of n = 1

Line	$I^{1/2}$	ν	δ	Line	$I^{1/2}$	ν	δ	Line	$I^{1/2}$	ν	δ
110-031	4.1	285.0	0.0	120-011	2.6	205.0	0.0	130-021	4.0	194.3	+0.1
110-131	2.7	69.4	-	121-030	3.9	193.4	0.0	130-121	0.41	6.4	-
111-020	3.5	278.6	+0.2	121-012	2.7	187.0	-	131-010	3.5	225.7	0.0
111-032	2.2	269.7	-0.1	122-031	5.2	197.4	-0.3	131-022	5.2	199.5	0.0
111-120	2.8	78.8	+0.2	122-013	3.8	172.9	+0.2	131-122	1.6	18.2	-
111-132	1.0	34.4	-	123-032	3.3	206.0	-0.1	132-011	2.2	249.4	-
112-021	3.0	263.2	0.0	123-014	2.6	163.0	0.0	132-023	3.2	209.7	0.0
112-033	1.8	244.6	+0.1	124-033	2.9	219.1	0.0	132-123	1.7	29.3	-
112-121	2.8	75.3	-0.2	124-015	2.3	157.9	-	133-012	2.1	274.4	0.0
113-022	5.4	248.9	0.0	125-034	3.4	236.2	0.0	133-024	2.7	223.3	0.0
113-034	2.3	219.3	+0.2	125-016	2.9	157.6	-	133-112	0.15	12.1	-
113-122	3.4	67.6	0.0	126-035	1.9	255.5	0.0	133-124	1.2	37.6	-
114-023	3.8	237.9	0.0	126-017	1.6	161.1	-	134-013	3.1	299.5	0.0
114-035	1.5	195.4	-	127-036	1.6	279.2	-0.1	134-025	3.2	238.4	-
114-123	2.0	57.5	-	127-018	1.4	170.9	+0.3	134-113	0.9	59.0	-
115-024	3.5	231.6	0.0	128-037	1.8	303.4	-	134-125	1.8	42.1	-
115-036	1.2	174.2	+0.3	128-019	1.4	183.2	-	135-014	2.4	318.3	0.0
115-124	1.4	45.9	-	128-137	0.3	36.0	-	135-026	1.7	248.2	+0.2

TABLE VI (continued)

Lines From the Levels of n = 1

Line	$I^{1/2}$	ν	δ	Line	$I^{1/2}$	ν	δ	Line	$I^{1/2}$	ν	δ
116-025	4.4	228.2	0.0	129-038	1.1	328.4	-	135-114	2.0	97.8	0.0
116-037	1.7	154.3	-	129-0110	0.8	198.0	-	135-126	0.8	37.7	-
116-125	1.3	31.9	-	129-138	0.5	82.4	-	136-015	2.5	317.1	0.0
117-026	2.7	231.5	-0.1	129-1110	0.2	5.4	-	136-027	1.1	238.3	-
117-038	1.1	139.9	0.0	1210-039	1.0	350.0	0.0	136-115	2.7	113.3	+0.1
117-126	0.5	21.0	-	1210-0111	0.5	210.5	-	136-127	0.18	8.3	
118-027	2.1	239.4	-0.1	1210-139	0.9	124.7	-	137-016	3.5	302.6	-0.3
118-039	0.9	129.5	+0.2					137-028	1.0	214.5	+0.3
118-127	0.3	9.4	-					137-116	3.5	113.1	+0.5
119-028	2.3	250.7	0.0					138-017	2.2	288.2	0.0
119-0310	1.0	122.7	-					138-029	0.6	189.6	-
1110-029	1.2	266.6	+0.1					138-117	2.1	106.1	0.0
1110-0311	0.5	121.5	-					139-018	2.0	276.1	0.0
								139-0210	0.4	165.2	-
								139-118	1.6	95.8	-
								1310-019	2.4	268.2	0.0
								1310-0211	0.5	143.1	0.1
								1310-119	0.9	84.8	-

TABLE VII.

Lines From the Levels of n = 2

Line	$I^{1/2}$	ν	δ	Line	$I^{1/2}$	ν	δ	Line	$I^{1/2}$	ν	δ
210-031	1.8	342.7	0.3	220-011	1.4	506.4	0.0	230-021	0.15	495.7	-
210-131	4.0	127.1	0.0	220-111	1.9	222.6	0.3	230-121	0.7	307.8	-0.1
211-020	0.1	360.6	-	220-211	3.2	140.5	0.0	231-010	2.2	474.7	0.0
211-032	1.7	351.7	0.0	221-030	0.1	546.0	-	231-022	0.2	448.5	-
211-120	1.8	160.8	-	221-012	1.2	539.6	0.0	231-110	4.6	179.6	-0.4
211-132	3.3	116.4	0.0	221-130	0.5	346.2	-0.3	231-122	0.9	267.2	0.1
212-021	0.1	392.6	-	221-112	1.2	277.3	-0.2	231-210	3.4	121.8	0.2
212-033	1.6	374.0	0.4	221-230	0.03	44.9	-	232-011	1.8	444.4	0.0
212-121	1.5	204.7	-	221-212	3.1	147.8	-0.1	232-023	0.2	404.7	-
212-133	3.1	117.3	0.0	222-031	0.1	599.1	-	232-111	4.1	160.6	-0.2
213-022	0.3	430.9	-	222-013	1.3	574.6	0.1	232-123	0.7	224.3	-
213-034	1.9	401.3	0.0	222-131	0.9	383.5	0.3	232-211	1.1	78.5	-
213-122	1.8	249.6	-	222-113	1.2	334.1	0.4	233-012	1.8	416.2	-0.1
213-134	3.8	123.0	0.1	222-231	0.3	134.5	-	233-024	0.1	365.1	-
213-234	0.5	30.4	-	222-213	3.8	152.1	-	233-112	4.2	153.9	0.1
214-023	0.2	473.5	-	223-032	0.8	617.6	0.0	233-124	0.8	179.4	-
214-035	1.1	431.0	0.0	223-014	.003	574.6	-	233-212	0.3	24.4	-
214-123	0.6	293.1	-0.3	223-132	0.9	382.3	-0.2	234-013	2.4	392.1	0.0

TABLE VII (continued)

Lines From the Levels of n = 2

Line	$I^{1/2}$	ν	δ	Line	$I^{1/2}$	ν	δ	Line	$I^{1/2}$	ν	δ
214-135	2.0	137.2	-	223-114	0.4	354.1	-	234-025	0.1	331.0	-
214-235	1.1	77.4	-	223-232	3.5	187.3	-0.1	234-113	5.5	151.6	0.1
215-024	0.1	519.6	-	223-214	0.1	118.5	-	234-125	1.3	134.7	
215-036	0.8	462.2	0.0	224-033	1.1	582.6	0.0	235-014	0.9	378.7	0.1
215-124	0.3	333.9	-	224-015	0.1	521.4	-	235-026	0.5	308.6	-
215-136	1.1	174.7	-	224-133	1.1	325.9	0.0	235-114	3.3	158.2	-
215-236	1.5	101.9	0.2	224-115	0.4	317.6	-	235-126	0.6	98.1	-
216-025	0.1	568.9	-	224-233	3.3	184.1	0.2	236-015	0.1	389.9	-
216-037	0.9	495.0	0.0	224-215	0.01	29.6	-	236-027	0.8	311.1	-0.1
216-125	0.5	372.6	-	225-034	1.5	548.6	-0.1	236-115	1.6	186.1	-
216-137	0.9	227.6	-	225-016	0.1	470.0	-	236-127	1.2	81.1	-
216-225	0.04	60.2	-	225-134	2.0	270.3	-	237-016	0.2	419.6	-
216-237	1.9	110.6	0.0	225-116	0.5	280.5	-	237-028	1.1	331.5	-0.3
217-026	0.04	620.5	-	225-234	4.4	177.7	0.1	237-116	1.3	230.1	-
217-038	0.5	528.9	-0.1	226-035	1.1	516.4	0.0	237-128	1.5	81.0	-
217-126	0.4	410.0	-	226-017	0.1	422.0	-	238-017	0.1	454.9	-
217-138	0.4	282.9	-	226-135	2.9	223.2	-0.1	238-029	0.6	356.3	-
217-226	0.1	149.1	-	226-117	0.3	239.9	-	238-117	0.5	272.8	0.0
217-238	1.1	116.2	-	226-235	2.2	162.8	-0.2	238-129	0.9	84.3	-

TABLE VII (continued)

Lines From the Levels of n = 2

Line	$I^{1/2}$	ν	ξ	Line	$I^{1/2}$	ν	ξ	Line	$I^{1/2}$	ν	ξ
218-027	0.2	659.5	-	227-036	1.1	486.1	0.0	239-018	0.1	496.0	-
218-039	0.2	549.6	-	227-018	0.1	377.8	-	239-0210	0.4	385.1	0.0
218-127	0.4	429.5	0.0	227-136	2.7	198.6	-	239-118	0.3	315.7	-
218-139	0.3	324.3	-	227-118	0.3	197.5	-	239-1210	0.7	95.2	-
218-227	0.3	222.6	-	227-236	1.0	125.8	-	239-2210	0.16	30.2	-
218-239	0.06	104.4	-	228-037	1.5	457.6	0.0	2310-019	0.1	540.8	-
219-028	0.7	623.9	0.0	228-019	0.1	337.4	-	2310-0211	0.4	415.7	-
219-0310	0.02	495.9	-	228-137	3.8	190.2	-0.1	2310-119	0.2	357.4	-
219-128	0.6	372.8	-	228-119	0.2	154.0	-				
219-1310	0.04	288.4	-	228-237	0.6	73.2	-				
219-228	2.7	219.2	0.1	229-038	0.9	432.6	-0.1				
219-2310	0.04	15.8	-	229-0110	0.03	302.2	-				
2110-029	0.5	590.1	-	229-138	2.2	186.6	-				
2110-129	0.5	318.1	-	229-1110	0.3	109.6	-				
2110-229	1.5	213.9	-0.2	229-238	0.1	19.9	-				
				2210-039	0.6	415.0	0.0				
				2210-0111	0.1	275.5	-				
				2210-139	1.6	189.7	-				

TABLE VIII.

Lines From the Levels of n = 3

Line	$I^{1/2}$	ν	ξ	Line	$I^{1/2}$	ν	ξ	Line	$I^{1/2}$	ν	ξ
310-131	0.2	822.2	-	320-011	0.1	746.9	-	330-021	0.5	736.2	-
311-020	0.3	980.4	-	320-111	0.2	463.1	-	330-121	0.7	548.3	-
311-120	0.6	780.6	-	321-030	0.9	694.6	-	330-221	2.9	195.7	0.0
311-320	2.1	238.7	-	321-012	0.1	688.2	-	331-010	0.1	807.0	-
312-021	0.2	924.7	-	321-130	0.8	494.8	-0.2	331-022	0.4	780.8	-
312-121	0.6	736.8	-	321-112	0.3	425.9	-	331-110	0.2	511.9	-
312-321	2.4	235.6	0.0	321-230	3.1	193.4	0.0	331-122	1.0	599.5	0.0
313-022	0.5	873.1	-	322-031	1.1	655.1	-	331-222	3.5	197.8	-
313-034	0.1	843.5	-	322-013	0.2	630.6	-	332-023	0.3	828.4	-
313-122	0.9	691.8	-	322-131	1.2	439.5	-0.1	332-111	0.1	584.3	-
313-134	0.1	565.2	-	322-113	0.3	390.1	-	332-123	0.6	648.0	-
313-322	3.5	234.1	0.0	322-231	4.8	190.5	0.2	332-323	2.1	199.9	-
314-023	0.4	824.8	-	323-032	0.1	654.5	-	333-024	0.2	879.1	-
314-123	0.6	644.4	-	323-014	0.5	611.5	0.0	333-124	0.5	693.4	-
314-135	0.1	489.3	-	323-132	0.3	419.2	-	333-324	1.7	201.8	-
314-223	2.5	232.8	0.0	323-114	0.6	391.0	-	334-025	0.2	931.9	-
315-024	0.4	779.3	-	323-214	2.3	155.4	0.0	334-125	0.6	735.6	-
315-124	0.6	593.6	-	324-033	0.1	710.7	-	334-325	1.9	202.9	0.0

TABLE VIII. (continued)

Lines from the Levels of n = 3

Line	$I^{1/2}$	ν	δ	Line	$I^{1/2}$	ν	δ	Line	$I^{1/2}$	ν	δ
315-136	0.1	434.4	-	324-015	0.4	649.5	-	335-014	0.1	1058.5	-
315-224	2.5	230.1	0.0	324-133	0.2	454.0	-	335-026	0.1	988.4	-
316-025	0.7	736.9	-	324-115	0.5	445.7	-	335-114	0.1	838.0	-
316-037	0.1	663.0	-	324-215	1.9	157.7	-	335-126	0.3	777.9	-
316-125	0.8	540.6	-0.3	325-034	0.1	768.9	-	335-326	1.0	205.9	-
316-137	0.2	395.6	0.3	325-016	0.4	690.3	-	336-015	0.1	1024.7	-
316-225	3.5	228.2	0.0	325-134	0.3	490.6	-	336-115	0.4	820.9	-
317-026	0.5	697.3	-	325-116	0.7	500.8	0.0	336-315	1.6	272.8	0.0
317-038	0.1	605.7	-	325-216	2.1	160.1	0.1	337-016	0.2	969.5	-
317-126	0.5	486.8	-	326-017	0.2	733.1	-	337-116	0.6	780.0	-
317-138	0.1	359.7	-	326-135	0.1	534.5	-	337-316	2.2	271.3	0.0
317-226	2.3	225.9	-	326-117	0.4	551.0	-	338-017	0.2	916.5	-
318-027	0.1	680.1	-	326-217	1.2	162.0	0.0	338-117	0.3	734.4	-
318-039	0.2	570.2	-	327-018	0.1	779.1	-	338-317	1.5	268.6	-
318-127	0.5	450.1	-	327-136	0.1	599.9	-	339-018	0.2	867.0	-
318-139	0.2	344.9	-	327-118	0.3	598.8	-	339-118	0.3	686.7	-
318-239	0.9	125.0	-	327-318	0.9	158.1	-	339-218	1.3	266.6	-
319-028	0.1	728.9	-	328-019	0.1	827.9	-	3310-019	0.3	821.2	-

TABLE VIII (continued)

Lines From the Levels of n = 3

Line	$I^{1/2}$	ν	δ	Line	$I^{1/2}$	ν	δ	Line	$I^{1/2}$	ν	δ
319-0310	0.2	600.9	-	328-119	0.3	644.5	-	3310-119	0.4	637.8	-
319-128	0.2	477.8	-	328-319	0.9	166.3	0.0	3310-219	1.7	264.6	-
319-1310	0.3	393.4	0.0	329-0110	0.1	879.6	-				
319-2310	0.6	120.8	-	329-1110	0.2	687.0	-				
3110-0311	0.1	640.0	-	329-3110	0.5	168.5	-				
3110-129	0.1	513.1	-								

tensity of a line is more nearly proportional to the square root of its true intensity than it is to the intensity itself. The unit in which $I^{1/2}$ is given is arbitrary since the figures listed are merely the product of the various factors, rotational, hindered rotational, nuclear spin enhancement, Boltzmann factor and frequency expressed in wave numbers. Lines with a calculated square root intensity of less than 0.1 were judged to be too faint to be observable in the present investigation and consequently are omitted from the tables. The third column gives the frequency obtained through the use of the $E_{obs.}$ appearing in Tables I to IV. The last column, δ, represents the difference between the frequency of column three

and the observed spectral line. A blank in this column results from one of three causes: (1) the line may have been too faint to have been observed, (2) the line may fall in a region overlaid by other stronger lines and be unresolved, or (3) the line falls outside the principal experimental region, namely from 50 to 625 cm^{-1}.

Figures 11–13 show the observed and predicted spectrum. In Figs. 11 and 12 the curve represents a composite of our observations supplemented by those of Oetjen and Palik. The short wavelength region also drew on the work of Borden and Barker. The relative intensities of the lines in any short portion of the spectrum are meaningful but not the comparison of the intensities of distant lines. This follows from the fact that the observations were made with a variety of different cell lengths and gas pressures with the view of obtaining maximum resolution in each region.

Above the observed spectrum are plotted the frequencies of Tables V–VIII. Each line is denoted by a triangle of height $I^{1/2}$. Since the triangles are similar, their areas are proportional to I. The intensity scale in Figs. 11 and 12 is doubled for all lines of frequency greater than 300 cm^{-1}.

Figure 13 is a tracing of the curve given by Borden and Barker (*1*) for the region 690 to 860 cm^{-1}. This portion of the spectrum was measured with a lesser degree of accuracy than that shown in Figs. 11 and 12 and in fact part of the region was completely obscured by the long wavelength CO_2 band since they did not use a vacuum spectrometer. It is presented merely to show that the theo-

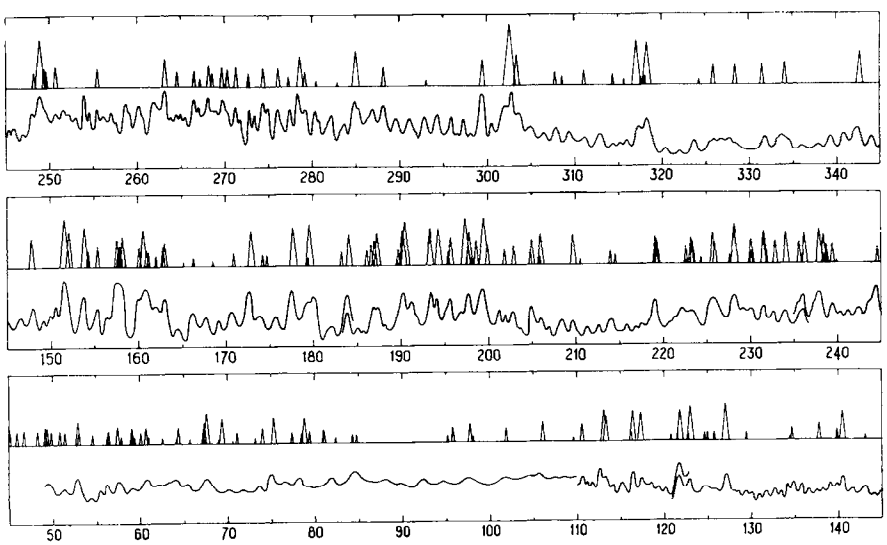

FIG. 11. Observed and calculated spectrum, ν/c = 45 to 345 cm^{-1}

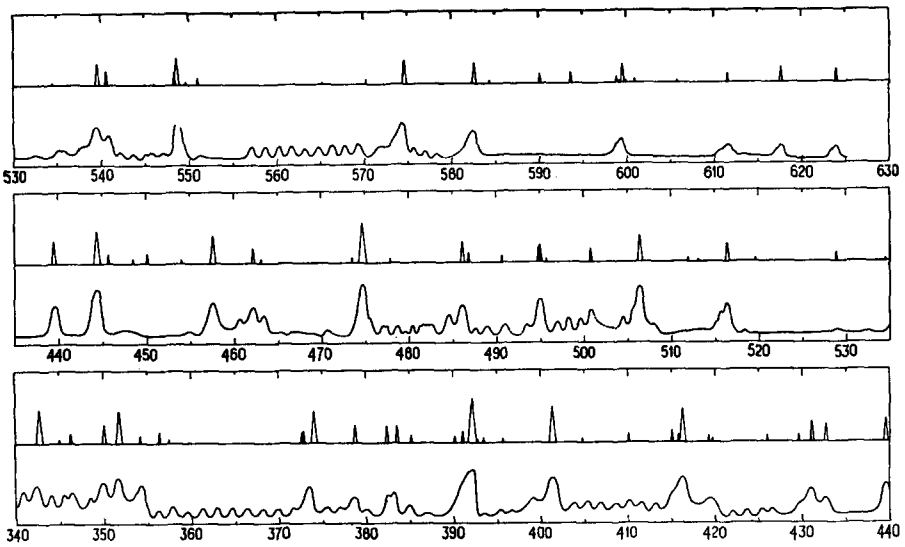

FIG. 12. Observed and calculated spectrum, ν/c = 340 to 630 cm^{-1}

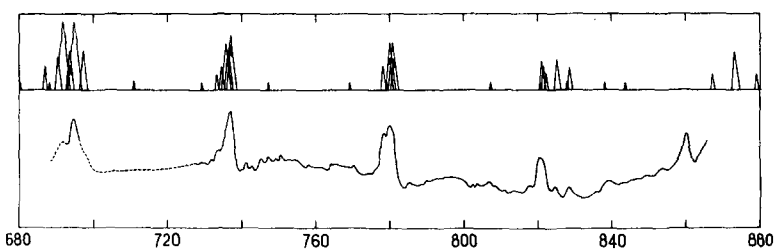

FIG. 13. Observed and calculated spectrum, ν/c = 690 to 860 cm^{-1}

retical lines are in general agreement with the observations but no attempt has been made to use it for the purpose of determining energy levels. The intensity scale of the predicted lines is five times greater than that employed in the 50 to 300 cm^{-1} region of Fig. 11.

In comparing the observed and predicted spectra the following points must be held in mind: (1) Every strong predicted line must correspond to a strong observed line. The only possible exceptions to this requirement may occur in strongly overlaid regions where many weak or medium strength lines may pile up and mask the existence of a single strong line. (2) Most of the strong observed lines must have associated predicted lines. This follows from the fact that the levels included in the present analysis, n = 0, 1, 2, 3 and K = 0 to 10 will account for virtually all of the intense transitions. However the requirements

under (2) are not as stringent as those of (1) since the accidental combinations of many weak lines could counterfeit the appearance of a strong line. (3) The positions of the observed and predicted lines must agree to within the limits of the convergences and perturbations which have been neglected. These have been estimated to be of the order of a few tenths of a cm^{-1}. (4) It is expected that many weak lines will be observed which are not predicted since the analysis only includes a limited number of states and moreover ignores the fine structure lines. It has been remarked that the sum of the intensities of all the fine structure lines is approximately twice the sum of the intensities of the lines being analyzed, namely the Q branch lines. Under the criteria just outlined the agreement between the observed and predicted spectra is good over most of the range and excellent in that part of the spectrum where the lines are well separated and hence well resolved.

A second test of self consistency involves the examination of possible combination relations. The selection rules are such that a pure combination relation requires four observed lines. An example is

$$[(113)-(022) = 248.9] + [(222)-(113) = 333.8] = 582.7 \text{ cm}^{-1}$$

and

$$[(131)-(022) = 199.3] + [(222)-(131) = 382.2] = 582.5 \text{ cm}^{-1}.$$

The number of these complete combinations is unfortunately not very large since in many cases at least one of the four lines is either too faint to be observed or is masked by other lines or falls outside of the experimental region. A second and somewhat less satisfactory type of combination relation is that in which there are two transitions starting from two different $n = 0$ levels and ending on the same excited level. Since the centrifugal corrections to the $n = 0$ levels, and in particular the difference in the corrections to nearby $n = 0$ levels, is small, one may place considerable trust in this type of combination. As an example

$$[(111)-(020) = 278.4] - [(111)-(032) = 269.8]$$
$$= 8.6 \text{ cm}^{-1} = (032)-(020) = 8.8 \text{ cm}^{-1}.$$

This last figure is obtained by subtracting the two energy levels in question appearing in Table I. One method of displaying the combination relations is to remark that many more lines have been identified in the spectrum than there are "observed" energy levels in Tables II–IV. There are in fact 145 identified lines from which 81 levels have been derived. For this reason the quantity δ appearing in Tables V–VIII is a valid measure of the degree to which the combination relations are fulfilled.

The third method of testing the uniqueness of the identifications of the lines may be described in the following way. Consider the $E_{\text{obs.}}$ for a particular value of n, say $n = 2$, which is listed in Table III. To each $E_{\text{obs.}}$ is added ΔE, (the

calculated centrifugal distortion correction) and from this is subtracted $3.4478K^2$, the overall rotational energy. The result is the unperturbed hindered rotational energy as determined from the observed spectrum. When plotted against K the points should lie on the analytic periodic curves shown in Fig. 1. The internal self consistency of these points which, it should be emphasized, are dependent upon the experimental spectrum can be made more evident in the following way. According to the theory the curves of hindered rotational energy are periodic functions of $\sigma = C_1K/C$ and repeat when σ increases by 3. The curves for $\tau = 2$ and $\tau = 3$ are identical with the $\tau = 1$ curve but have been displaced to the left or to the right, respectively, by the amount $\sigma = 1$. Thus by a proper transformation all points may be displayed on the curve of $\tau = 1$. One may make a further contraction by noticing that the curve of $\tau = 1$ is symmetrical about $C_1K/C = 1.5$. All points may therefore be plotted on the single section of curve from $\sigma = 0$ to 1.5. This has been done in Fig. 14 for the observed levels of $n = 2$ and it is clear that the points appear to fall on an analytic curve in conformity

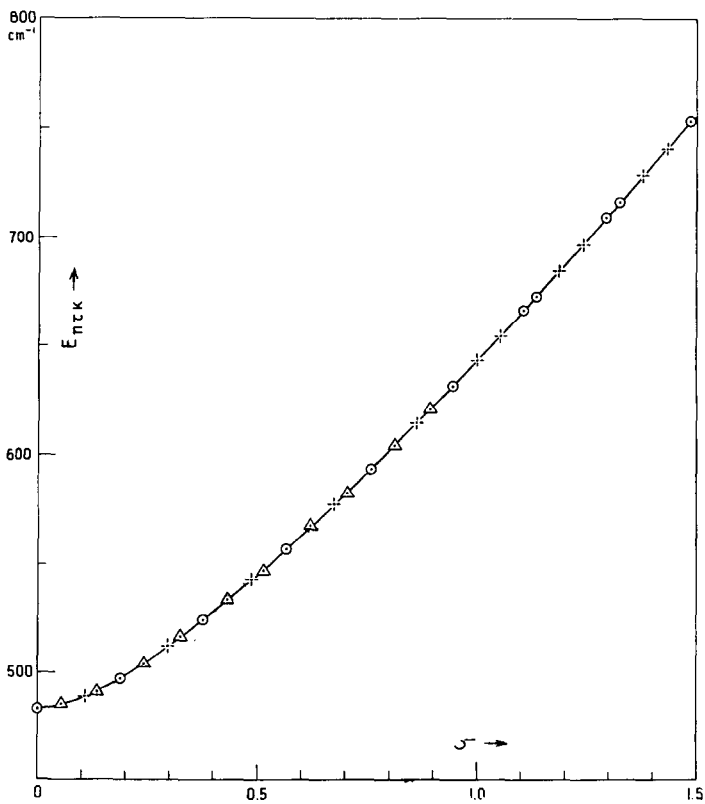

FIG. 14. Observed internal rotational levels for $n = 2$ plotted against σ

with the requirements of the theory. The scale of Fig. 14 is however rather small and deviations of the order of one wave per centimeter or less are not readily apparent.

To obviate this difficulty one may now subtract from the ordinate of each point the calculated value of the hindered rotation and then replot. The result of this procedure is shown in Fig. 15 for the levels of $n = 1, 2$ and 3. The number appearing above each point represents the K value of the level. The final ordinates of Fig. 15 are of course equal to the difference between the $E_{\text{obs.}}$ and $E_{\text{calc.}}$ of the tables but an advantage is gained by displaying them with the single abscissa scale of σ which runs from 0 to 1.5.

A complete agreement between theory and experiment would result in all points falling on horizontal lines of ordinate 0.0. Deviations of the points from these lines may arise from the following causes: (1) An irregular scatter will result from experimental errors and from neglect of the various convergences affecting the positions of the Q branch lines. These have been estimated to be of the order of a few tenths of a wave per centimeter and an inspection of Fig. 15

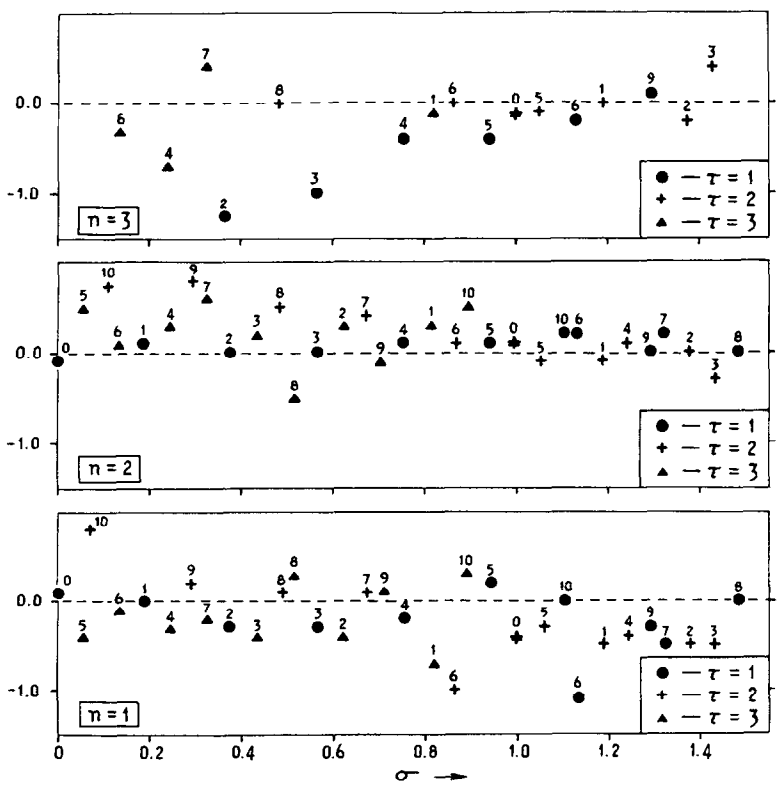

FIG. 15. $E_{\text{obs.}} - E_{\text{calc.}}$ plotted against σ

shows that the points of $n = 1$ and 2, where the data are best, do indeed exhibit this order of scatter. Certain points however show rather large deviations; for example those relating to the levels (116), (126), and (238). It is possible that these may be due to an accumulation of small errors or perhaps to accidentally large asymmetry contributions. These latter could occur for near resonances between unperturbed levels. (2) The corrections for centrifugal distortion depend upon both K and τ. Thus an improper correction would tend to separate the points into the three groups corresponding to $\tau = 1$, 2 and 3. There is some indication of such a separation in the points of $n = 2$ in the region $\sigma = 0$ to 0.6 but for the most part the points with different τ values seem quite well mixed. (3) The hindering potential has been assumed to have the form $\frac{1}{2}H(1 - \cos 3x)$ with $H = 374.82$ cm^{-1}. If however the potential is not sinusoidal one might think to develop it in a Fourier series in the variable $3x$. It would be convenient to express the next term in the expansion as $G(1 - \cos 6x)$. A slight readjustment in the barrier height might be necessary. These perturbations in the potential would then give a correction to the energy levels of amount

$$G\langle(1 - \cos 6x)\rangle + \tfrac{1}{2}\Delta H\langle(1 - \cos 3x)\rangle.$$

A calculation of this correction was made in the hope that a proper choice of the constants G and ΔH might bring the points of Fig. 15 closer to the 0.0 ordinate. The improvement thus obtained was so slight as not to be significant. One definite conclusion did emerge however. The constant G can not be greater than one or two wave numbers without significantly disturbing the agreement and consequently the hindering potential in methanol must be sinusoidal to better than one percent accuracy.

APPENDIX

The internal rotation wave functions of the symmetrical rotator are denoted by,

$$P_{n\tau K} = (2\pi)^{-1/2} \sum_{\rho=-\infty}^{\infty} a_\rho \exp(i\rho x),$$

where the normalization factor $(2\pi)^{-1/2}$ has been included so that

$$\int_0^{2\pi} P^*_{n\tau K} P_{n\tau K}\, dx = \sum_{-\infty}^{\infty} a_\rho^2 = 1.$$

In the following tables, for convenience, the a_ρ as listed have been multiplied by 10^4. Only those a_ρ are included which are large enough to make significant contributions in the calculation of matrix elements. The Fourier coefficients for the $n = 3$ levels are also omitted. These levels lie so high above the potential barrier that the coefficients may be readily evaluated through the perturbation formulas given by Hecht and Dennison (*11*) in Appendix I.

RECEIVED: October 20, 1958

Table IX. $a_p \times 10^4$ for $n = 0$ $\tau = 1$

K =	0	1	2	3	4	5	6	7	8	9	10
a_{-9}=	10	8	7	6	5	4	3	2	2	2	1
a_{-6}=	254	216	184	156	133	112	94	77	63	50	39
a_{-3}=	2857	2571	2316	2083	1867	1660	1459	1263	1074	899	745
a_0 =	9140	9117	9044	8914	8714	8427	8037	7536	6939	6283	5619
a_3 =	2857	3184	3561	3998	4504	5081	5717	6383	7034	7618	8102
a_6 =	254	301	359	431	521	632	766	924	1101	1292	1489
a_9 =	10	13	16	20	25	32	41	52	65	80	96

Table X. $a_p \times 10^4$ for $n = 0$ $\tau = 2$

K =	0	1	2	3	4	5	6	7	8	9	10
a_{-7}=	107	89	73	59	47	37	29	23	18	14	11
a_{-4}=	1603	1403	1208	1023	853	705	581	480	398	333	266
a_{-1}=	8328	7906	7356	6757	6094	5436	4823	4276	3801	3391	2922
a_2 =	5256	5904	6571	7208	7766	8219	8563	8810	8978	9081	9149
a_5 =	668	809	973	1154	1347	1546	1749	1959	2182	2423	2756
a_8 =	34	44	55	69	84	102	121	143	168	197	240

Table XI. $a_p \times 10^4$ for $n = 0$ $\tau = 3$

K =	0	1	2	3	4	5	6	7	8	9	10
a_{-8}=	34	27	21	17	14	11	9	7	6	5	4
a_{-5}=	668	550	455	378	316	267	226	192	164	139	118
a_{-2}=	5256	4661	4134	3678	3285	2945	2656	2385	2147	1927	1718
a_1 =	8328	8642	8865	9014	9102	9139	9155	9070	8958	8779	8518
a_4 =	1603	1808	2021	2248	2496	2772	3001	3448	3867	4354	4910
a_7 =	107	127	150	176	206	242	278	341	409	493	598

Table XII. $a_\rho \times 10^4$ for n = 1 τ = 1

K =	0	1	2	3	4	5	6	7	8	9	10
a_{-9} =	41	21	12	8	6	5	4	4	3	3	3
a_{-6} =	870	465	280	200	158	134	119	109	101	94	88
a_{-3} =	7017	4120	2744	2145	1848	1692	1609	1565	1537	1511	1478
a_0 =	0	1944	2914	3589	4216	4866	5554	6262	6950	7572	8092
a_3 =	-7017	-8812	-9070	-8982	-8765	-8447	-8021	-7485	-6851	-6156	-5449
a_6 =	- 870	-1172	-1280	-1345	-1398	-1444	-1484	-1515	-1541	-1570	-1618
a_9 =	- 41	- 57	- 65	- 71	- 76	- 82	- 89	- 95	- 102	- 110	- 121

Table XIII. $a_\rho \times 10^4$ for n = 1 τ = 2

K =	0	1	2	3	4	5	6	7	8	9	10
a_{-7} =	129	116	106	99	92	86	80	74	68	45	52
a_{-4} =	1663	1594	1556	1530	1502	1468	1425	1376	1319	897	1080
a_{-1} =	5058	5755	6462	7135	7730	8219	8597	8871	9040	6522	8351
a_2 =	-8337	-7882	-7314	-6658	-5955	-5252	-4580	-3944	-3310	-1847	-1260
a_5 =	-1456	-1478	-1523	-1548	-1581	-1639	-1748	-1953	-2351	-2306	-5208
a_8 =	- 84	- 90	- 97	- 104	- 113	- 125	- 143	- 174	- 228	- 246	- 610

Table XIV. $a_\rho \times 10^4$ for n = 1 τ = 3

K =	0	1	2	3	4	5	6	7	8	9	10
a_{-8} =	84	78	72	66	60	47	25	14	9	6	5
a_{-5} =	1456	1412	1361	1300	1212	989	556	317	217	168	140
a_{-2} =	8338	8685	8931	9063	8957	7799	4790	3019	2272	1914	1727
a_1 =	-5058	-4397	-3767	-3118	-2280	- 672	1524	2688	3408	4038	4678
a_4 =	-1663	-1793	-2040	-2526	-3597	-6099	-8554	-9054	-9023	-8837	-8547
a_7 =	- 129	- 150	- 186	- 251	- 394	- 738	-1118	-1257	-1328	-1384	-1432
a_{10} =	- 5	- 6	- 7	- 10	- 17	- 34	- 54	- 63	- 69	- 75	- 81

Table XV. $a_\rho \times 10^4$ for $n = 2$ $\tau = 1$

K =	0	1	2	3	4	5	6	7	8	9	10
a_{-9}=	41	50	49	47	44	42	39	37	13	1	1
a_{-6}=	861	1084	1103	1080	1049	1017	986	955	338	32	19
a_{-3}=	6407	8660	9262	9478	9590	9660	9710	9744	3594	382	247
a_0 =	-4053	-3616	-3112	-2761	-2499	-2291	-2118	-1966	366	341	468
a_3 =	6407	3243	1792	1148	804	594	449	320	-1628	-1989	-2142
a_6 =	861	488	314	243	215	216	257	429	9134	9746	9703
a_9 =	41	25	17	14	14	15	20	36	869	960	990

Table XVI. $a_\rho \times 10^4$ for $n = 2$ $\tau = 2$

K =	0	1	2	3	4	5	6	7	8	9	10
a_{-7}=	1008	977	946	89	26	17	14	14	15	20	31
a_{-4}=	9676	9721	9746	981	320	232	212	223	266	371	628
a_{-1}=	-2239	-2073	-1922	171	378	507	674	931	1373	2267	4406
a_2 =	548	413	268	-1867	-2030	-2190	-2376	-2604	-2898	-3308	-3870
a_5 =	222	282	584	9728	9731	9690	9633	9548	9405	9086	8010
a_8 =	16	22	51	935	968	999	1031	1063	1091	1104	1030

Table XVII. $a_\rho \times 10^4$ for $n = 2$ $\tau = 3$

K =	0	1	2	3	4	5	6	7	8	9	10
a_{-8}=	16	14	14	16	22	36	49	50	47	45	42
a_{-5}=	222	212	232	287	422	743	1054	1105	1088	1058	1026
a_{-2}=	548	735	1030	1560	2691	5378	8281	9157	9433	9564	9643
a_1 =	-2239	-2436	-2680	-3000	-3454	-4001	-3784	-3236	-2849	-2567	-2346
a_4 =	9676	9612	9516	9342	8913	7321	3957	2083	1288	884	645
a_7 =	1008	1040	1071	1098	1099	960	574	349	257	220	213
a_{10}=	41	43	46	48	50	46	29	19	15	14	14

REFERENCES

1. A. Borden and E. F. Barker, *J. Chem. Phys.* **6,** 553 (1938).
2. J. S. Koehler and D. M. Dennison, *Phys. Rev.* **57,** 1004 (1940).
3. W. D. Hershberger and J. Turkevich, *Phys. Rev.* **71,** 554 (1947).
4. R. H. Hughes, W. E. Good, and D. K. Coles, *Phys. Rev.* **84,** 418 (1951).
5. D. G. Burkhard and D. M. Dennison, *Phys. Rev.* **84,** 408 (1951).
6. E. V. Ivash and D. M. Dennison, *J. Chem. Phys.* **21,** 1804 (1953).
7. H. M. Randall and F. Firestone, *Rev. Sci. Instr.* **9,** 404 (1938).
8. N. Fuson, thesis, University of Michigan, 1939.
9. H. M. Randall, D. M. Dennison, N. Ginsburg, and L. R. Webber, *Phys. Rev.* **52,** 160 (1937).
10. S. L. Gerhard and D. M. Dennison, *Phys. Rev.* **43,** 197 (1933).
11. K. T. Hecht and D. M. Dennison, *J. Chem. Phys.* **26,** 48 (1957).
12. T. Chang, thesis, University of Michigan, 1954, p. 46.